Molecular Microbiology (2015) 96(6), 1159–1175

doi:10.1111/mmi.12999
First published online 11 April 2015

Expression of the glycolytic enzymes enolase and lactate dehydrogenase during the early phase of *Toxoplasma* differentiation is regulated by an intron retention mechanism

Matteo Lunghi,[1†] Roberto Galizi,[2†] Alessandro Magini,[1] Vern B. Carruthers[3] and Manlio Di Cristina[1*‡]

Departments of [1]Chemistry, Biology and Biotechnology, and [2]Experimental Medicine, University of Perugia, Perugia, Italy.

[3]Department of Microbiology and Immunology, University of Michigan Medical School, Ann Arbor, MI, USA.

Summary

The intracellular parasite *Toxoplasma gondii* converts from a rapidly replicating tachyzoite form during acute infection to a quiescent encysted bradyzoite stage that persists inside long-lived cells during chronic infection. Bradyzoites adopt reduced metabolism and slow replication while waiting for an opportunity to recrudesce the infection within the host. Interconversion between these two developmental stages is characterized by expression of glycolytic isoenzymes that play key roles in parasite metabolism. The parasite genome encodes two isoforms of lactate dehydrogenase (LDH1 and LDH2) and enolase (ENO1 and ENO2) that are expressed in a stage-specific manner. Expression of different isoforms of these enzymes allows *T. gondii* to rapidly adapt to diverse metabolic requirements necessary for either a rapid replication of the tachyzoite stage or a quiescent lifestyle typical of the bradyzoites. Herein we identified unspliced forms of LDH and ENO transcripts produced during transition between these two parasite stages suggestive of an intron retention mechanism to promptly exchange glycolytic isoforms for rapid adaptation to environmental changes. We also identified key regulatory elements in the ENO transcription units, revealing cooperation between the ENO2 5′-untranslated region and the ENO2 intron, along with identifying a role for the ENO1 3′-untranslated region in stage-specific expression.

Accepted 11 March, 2015. *For correspondence. E-mail manlio.dicristina@unipg.it; Tel. (+39) 075 5857443; Fax (+39) 075 585 7436. †These authors contributed equally to this work. ‡Present address: Department of Chemistry, Biology and Biotechnology, University of Perugia, via del Giochetto, Perugia 06122, Italy.

Introduction

Toxoplasma gondii is a highly successful parasite capable of infecting all warm-blooded vertebrates including ~ 30% of the total human population. Its success relies on effective routes of transmission and an ability to avoid causing severe disease by differentiating from a rapidly replicating tachyzoite form to a slow dividing bradyzoite form. Whereas tachyzoites elicit a vigorous immune response, semi-dormant bradyzoites persist virtually unscathed in the host, residing indefinitely inside cysts harbored within several types of host cells including myocytes and neurons (Dubey *et al.*, 1998; Weiss and Kim, 2000). Tachyzoites and bradyzoites are further distinguished by having disparate energy requirements that reflect large differences of their metabolism. Tachyzoites utilize glycolysis as a major source of energy, generating lactate as the main product. The tricarboxylic acid (*TCA*) cycle metabolism also contributes substantially to energy production in this parasite stage. On the other hand, bradyzoites seem to lack a functional TCA cycle and respiratory chain (Denton *et al.*, 1996) and rely on catabolism of starch in amylopectin granules for energy production. So, glycolysis is necessary for energy production in both tachyzoites and bradyzoites, although it seems to be the predominant pathway in bradyzoites (Bohne *et al.*, 1999). The parasite adapts to these metabolic differences by expressing different sets of glycolytic enzymes. Two key enzymes of glycolysis, lactate dehydrogenase (LDH) and enolase (ENO), are differentially expressed in tachyzoites and bradyzoites (Tomavo, 2001; Weiss and Kim, 2013). LDH is a glycolytic enzyme that converts pyruvate to lactate and plays an indispensable role when glycolysis becomes the only pathway to provide energy under anaerobic conditions (Kavanagh *et al.*, 2004). Two copies of this enzyme are present in *Toxoplasma* genome, *LDH1* and *LDH2*, which are exclusively expressed in tachyzoites and bradyzoites respectively (Yang and Parmley, 1995; 1997). LDH2 activity is about three times higher than

LDH1, probably because of bradyzoite dependence on amylopectin catabolism (Denton *et al*., 1996). Moreover, the LDH2 bradyzoite-specific isoenzyme is resistant to acidic pH, allowing bradyzoites to tolerate acidification resulting from amylopectin catabolism to lactate. Stage-specific knockdown of LDH1 or LDH2 impaired parasite replication and resulted in a significant reduction of brain cyst burden in a murine model (Al-Anouti *et al*., 2004), indicating important contributions of these isoenzymes to infection.

The other key glycolytic enzyme, ENO, is also expressed in two stage-specific isoforms, termed ENO1 and ENO2 in bradyzoites and tachyzoites respectively (Manger *et al*., 1998; Yahiaoui *et al*., 1999; Dzierszinski *et al*., 2001; Kibe *et al*., 2005). ENO converts 2-phosphoglycerate to phosphoenolpyruvate, and the tachyzoite-specific isoform ENO2 displays a threefold greater catalytic rate than the bradyzoite isoform ENO1. The higher activity of ENO2 might reflect the higher energy requirement of tachyzoites due to their rapid growth rate. However, ENO1 is more thermo-stable than the tachyzoite isoform, a feature that may confer higher resistance to increased stress (Tomavo, 2001). Moreover, Ferguson *et al*. reported that a subpopulation of both ENO isoforms resides in the parasite nucleus during early intracellular proliferation and development (Ferguson *et al*., 2002). ENO1 nuclear localization seems to be dependent on ENO2 expression because silencing of this latter alters nuclear targeting of ENO1 (Holmes *et al*., 2010). Very recently, a new study showed that these ENOs are associated with nuclear chromatin and regulate gene expression of numerous gene targets (Mouveaux *et al*., 2014). This study also showed that genetic ablation of ENO1 reduced the number of brain cysts in chronically infected mice and altered expression of several genes in bradyzoites. These new data suggest that ENO genes play key roles during tachyzoite-bradyzoite interconversion by regulating genes involved in differentiation.

Several reports show that expression of key cellular factors may also be regulated by posttranscription mechanisms such as time-regulated splicing (Averbeck *et al*., 2005; Xu *et al*., 2008; Yap *et al*., 2012; Boothby *et al*., 2013; Zhan, 2013). Among these processes, intron retention (IR) is a type of alternative splicing exploited by cells to provide messengers that cannot be translated until a stimulus triggers splicing of the regulated intron(s), licensing these messengers to produce their coded product (Boothby *et al*., 2013).

Herein we provide experimental evidence that expression of LDH and ENO isoforms is subjected to posttranscriptional control. Our findings show for the first time that parasites regulate splicing to produce unspliced LDH and ENO transcripts as a prelude to interconversion. Our results indicate that *Toxoplasma* exploits an intron-retention mechanism to prevent synthesis of the glycolytic enzymes from transcripts generated during the early phase of the differentiation process. Furthermore, we dissected ENO transcription units to identify the elements involved in the posttranscriptional regulation of *ENO* genes.

Results

IR precludes expression of glycolytic enzyme isoforms at an inappropriate stage

Tachyzoite-specific LHD1 and ENO2 and bradyzoite-specific LDH2 and ENO1 each contain a single intron near the 5′ end of their respective coding sequences (Fig. 1A). Using ENO1 as bradyzoite marker in reverse transcription-polymerase chain reaction (RT-PCR) experiments, we identified in cDNA prepared from *in vitro* ($_{i}$Tz) and *in vivo* ($_{p}$Tz) tachyzoites of PLK strain *T. gondii* a 1.2 kb PCR product consistent with an unspliced form of ENO1 (Fig. 1B, lanes 4 and 6 respectively). Sequencing this PCR product confirmed that it was effectively the unspliced form of ENO1 containing in-frame stop codons within the intron. PCR of the corresponding nonreversed transcribed RNAs showed no amplification, ruling out that the product originated from genomic DNA contamination. cDNA generated from *T. gondii* PLK bradyzoite cysts (Bz) isolated from infected mouse brains exclusively showed the spliced form of ENO1 (Fig. 1B, lane 2), indicating that unspliced transcripts were specific to the tachyzoite stage or potentially the transitional phase during tachyzoite-bradyzoite interconversion. Weak expression of the mature form of ENO1 was also seen in PLK tachyzoites (Fig. 1B, lanes 4 and 6), perhaps due to the presence of a few spontaneously converted bradyzoites occurring during normal growth of this cystogenic strain *in vitro* and *in vivo*. The unspliced form of ENO1 was the only PCR product detectable in cDNA generated from tachyzoite mRNAs of the poorly cystogenic strain RH (Fig. 1C, lane 2). Spontaneous conversion of this type I RH strain in *in vitro* cultures is very low or even absent, suggesting that IR occurred in the tachyzoite stage. Similar to ENO1, the bradyzoite-specific LDH2 transcript showed IR in tachyzoites (Fig. 1D), as confirmed by sequencing the PCR product. Together, these results indicate that unspliced transcripts of bradyzoite-specific ENO1 and LDH2 are present in tachyzoites, suggesting an IR mechanism that precludes expression of these proteins at an inappropriate stage.

To investigate the extent that IR also occurs in bradyzoites, we converted tachyzoites to *in vitro* bradyzoites (iBz) for 10 days in alkaline culture medium and prepared cDNA from the resulting differentiated parasites. Because *in vitro* conversion is not 100% efficient, the cultures are enriched for bradyzoites, but also contain tachyzoites and parasites in transition between the two stages. Detection

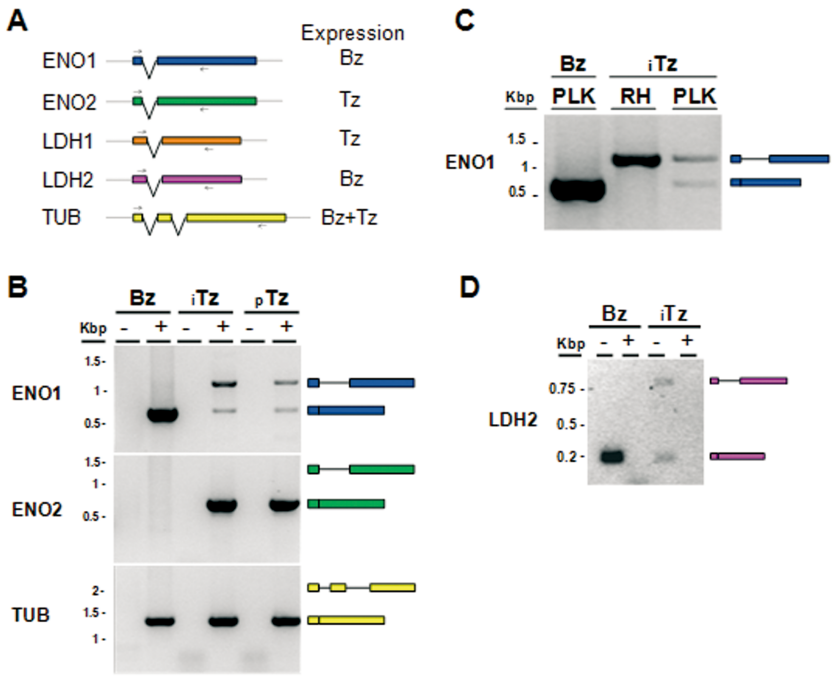

Fig. 1. IR in ENO1 and LDH2 transcripts during the tachyzoite stage.
A. Schematic representation of the genes and primers used in the study. Exons are represented as rectangles whereas introns are indicated with lines linking the exons. Primers are indicated by arrows.
B. Agarose gel electrophoresis of RT-PCR products from RNA isolated from PLK cysts (Bz), *in vitro* tachyzoites (iTz) or intraperitoneal tachyzoites (pTz) using primers E1F/E1R (top panel), E2F/E2R (middle panel) or T5F/T5R (bottom panel). Schematic representations of the expected amplification products of unspliced and spliced transcripts are indicated to the right of each gel. Positive ('+') and negative ('–') signs indicate RNAs with or without reverse transcriptase respectively.
C. Only the unspliced form of ENO1 is detected in cDNA generated from RH tachyzoite RNA. Agarose gel electrophoresis of RT-PCR products from RNA using E1F and E1R primers.
D. LDH2 transcripts show IR in *in vitro* PLK tachyzoites (iTz) but not in *in vitro* bradyzoites (iBz). RT-PCR was performed using primers L2F/L2R to detect LDH2 transcripts.

of the tachyzoite-specific SAG1 transcript confirmed that the differentiated cultures contain a mixture of stages (Fig. 2A, upper panel lane 2). Further analysis of iBz samples showed that unspliced transcripts of tachyzoite-specific LDH1 and ENO2 are present in bradyzoites, the stage in which they are not expressed (Fig. 2A upper panel lane 3 and Fig. 2B upper panel lane 1 respectively). In contrast, unspliced transcripts of LDH1 and ENO2 were absent from *in vitro* tachyzoites, the stage in which they are expressed (Fig. 2A bottom panel lane 3 and Fig. 2B upper panel lane 3 respectively). Collectively, our findings suggest that IR occurs in both tachyzoites and bradyzoites to impede expression of ENO and LDH isoforms at an unsuited stage.

Appropriate expression of ENO2 in tachyzoites depends on the ENO2 intron

To identify elements of the *ENO2* gene that regulate synthesis of this glycolytic enzyme, we designed a series of

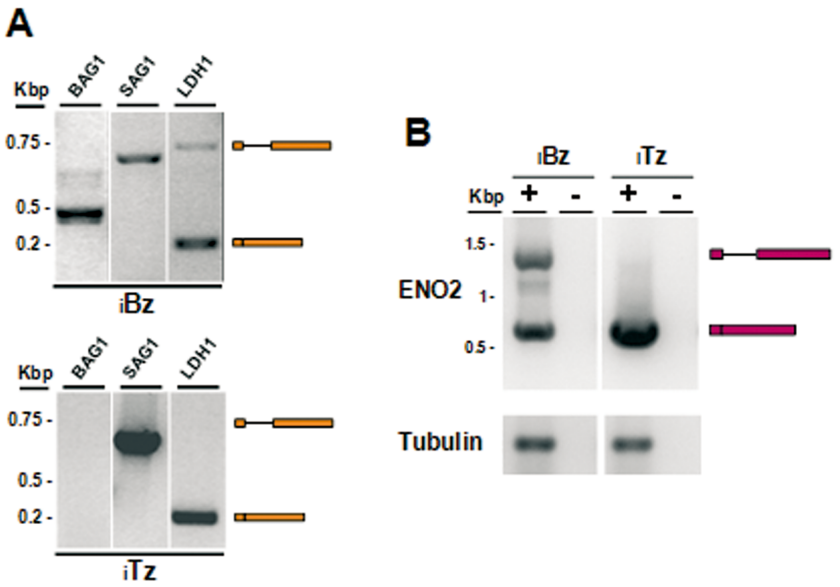

Fig. 2. LDH1 and ENO2 transcripts show IR in *in vitro* differentiated bradyzoites.
A. Analysis of LDH1 expression and splicing. Total RNAs were isolated from either *in vitro* PLK tachyzoites (iTz) or PLK parasites grown in HFF cells with alkaline media (pH 8.2) for 6 days (iBz) and analyzed by RT-PCR using primers to detect BAG1 (bradyzoite marker, B1F and B1R primers), SAG1 (tachyzoite marker, S1F and S1R primers) and LDH1 (L1F and L1R primers) transcripts. Minus reverse transcriptase control for each set of primers was performed but not shown in the figure.
B. Analysis of ENO2 expression and splicing. RNA isolation and RT-PCR was performed as in A with E2F and E2R or T5F and T5R primers.

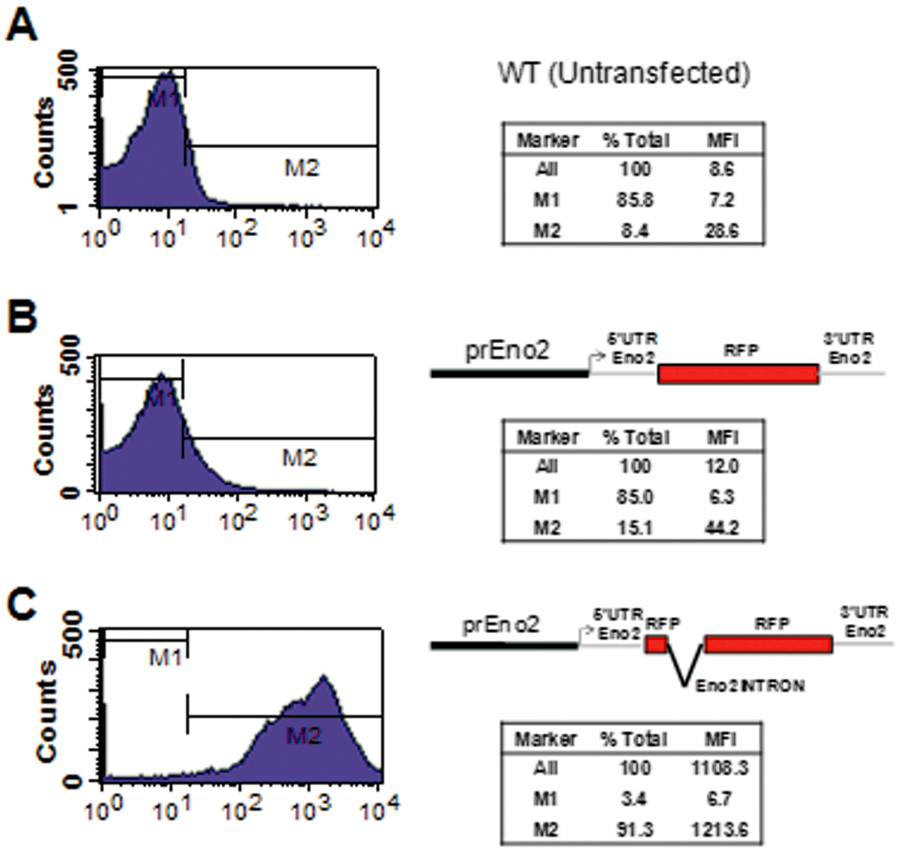

Fig. 3. The ENO2 transcription unit requires an intron to express RFP. PLK tachyzoites were analyzed as WT parasites (A) or were stably transfected with either *prENO2/RFP* (B) or *prENO2/RFP + INT$_{ENO2}$* (C) along with a DHFR resistance cassette. After 8 days of pyrimethamine selection, stably transfected populations were analyzed by flow cytometry. There were 100 000 events counted for each strain. Data are from one representative experiment out of three with similar results. MFI, mean fluorescence intensity.

red fluorescent protein (RFP) reporter constructs to dissect the main constituents of the ENO2 expression unit in stably transfected PLK strain. The basal construct, named *prENO2/RFP*, carries a fragment spanning 1930 bp upstream of the ENO2 start codon to drive expression of RFP (lacking introns) followed by a 683 bp fragment downstream of the ENO2 stop codon. This construct was designed based on the largest construct described by Kibe *et al*. (2005). Transfection of PLK tachyzoites using 100 μg of the prENO2/RFP vector resulted in low expression of RFP after 24 h, with few tachyzoites displaying a barely detectable fluorescence by microscopy (data not shown). After 8 days of pyrimethamine selection, stable parasite populations carrying prENO2/RFP vector were analyzed by flow cytometry. This analysis showed that RFP was poorly expressed and in a low percentage of prENO2/RFP transfected parasites (Fig. 3B) that was only marginally higher than WT (untransfected) parasites (Fig. 3A). This result was in accordance with that reported in Kibe *et al.*'s manuscript where the authors stated that, based on CAT expression, both *ENO* genes exhibited weak promoter activity (Kibe *et al*., 2005). So, taking in consideration results on IR obtained above, we wondered whether the ENO2 intron might have an influence on ENO2 expression. To assess this, we generated a new construct, named *prENO2/RFP + INT$_{ENO2}$*, in which the ENO2 intron was placed 40 bp downstream of the ATG of RFP coding region, mirroring the exogenous gene. An analysis of RFP fluorescence either 24 h posttransfection or 8 days postpyrimethamine selection showed that RFP expression was restored by the presence of the ENO2 intron with tachyzoites displaying strong fluorescence intensity (Fig. 3C). Thus, these findings suggest the ENO2 intron as a key element for efficient expression from the ENO2 transcription unit.

The ENO2 5′UTR suppresses RFP expression in absence of the ENO2 intron

To understand the basis of the ENO2 intron requirement for RFP expression, we first investigated whether the intron contained a transcription enhancer. We assessed if the

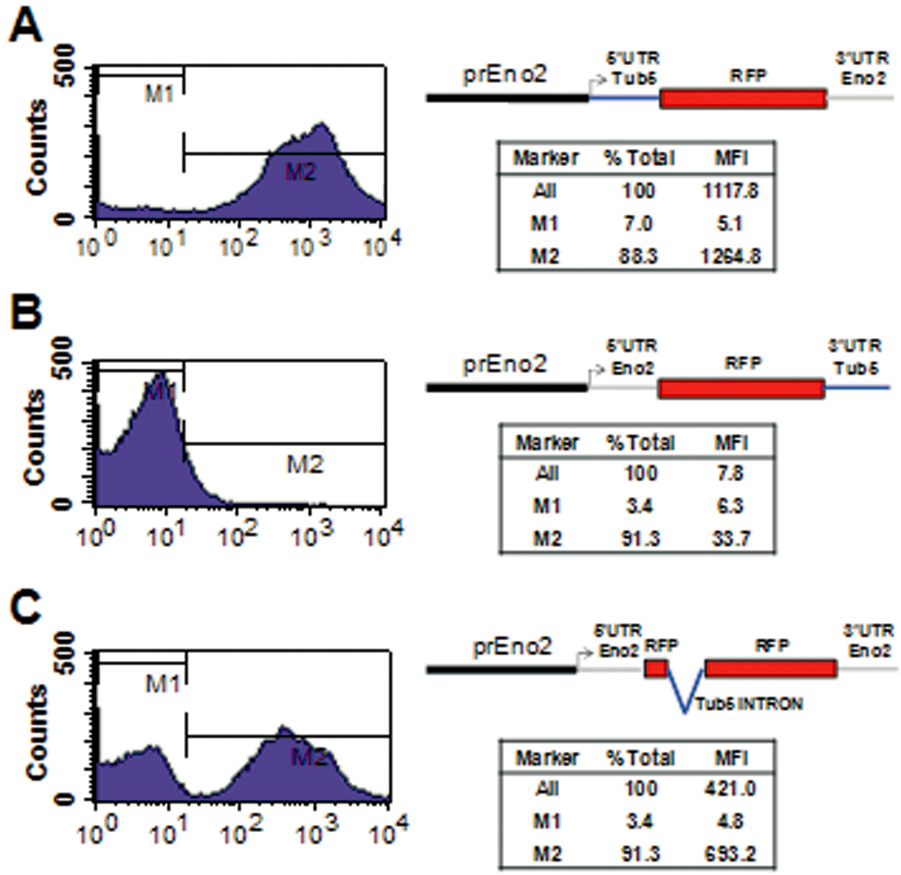

Fig. 4. The ENO2 5′ UTR suppresses RFP expression in the absence of an intron. PLK tachyzoites were stably transfected with *prENO2/5′UTR$_{TUB}$-RFP* (A), *prENO2/RFP-3′UTR$_{TUB}$* (B) or *prENO2/RFP + INT$_{TUB}$* (C) along with DHFR resistance cassette. After 8 days of pyrimethamine selection, stable transfected populations were analyzed by flow cytometry. There were 100 000 events counted for each transgenic tachyzoites. Untransfected tachyzoites were also analyzed to assess autofluorescence (data not shown). Data are from one representative experiment out of three with similar results. MFI, mean fluorescence intensity.

ENO2 intron was capable of conferring expression in a construct containing the SAG1 promoter lacking its transcriptional activation region by replacing the ENO2 promoter and 5′UTR of *prENO2/RFP + INT$_{ENO2}$* with a sequence beginning 70 bp upstream of the SAG1 transcription start sites. This fragment of the SAG1 promoter was already shown to be insufficient to drive transcription of CAT reporter (Soldati and Boothroyd, 1995), requiring at least two of the five 27 repeats placed upstream of the –70 bp region of SAG1. Transfection with this construct showed no RFP expression (data not shown), making it unlikely that the ENO2 intron contains a transcriptional enhancer.

Next we investigated whether the absence of the ENO2 intron suppresses RFP expression in a manner dependent on another element in the transcription unit by generating a series of constructs composed of different assemblies of ENO2 or Tub5 UTRs. Two new constructs were derived from *prENO2/RFP*, in which either the ENO2 5′ UTR (*prENO2/5′UTR$_{TUB}$-RFP*) or 3′ UTR (*prENO2/RFP-3′UTR$_{TUB}$*) were replaced with those of *Toxoplasma* tubulin gene. Interestingly, 5′-UTR replacement resulted in expression of RFP (Fig. 4A) whereas the 3′-UTR exchange had no effect (Fig. 4B). These results indicated that: (i) the ENO2 5′UTR suppresses expression in the absence of an intron; and (ii) the ENO2 promoter has intrinsic transcriptional activity and does not require the presence of its intron to produce transcripts. To confirm these data, we also generated two other constructs carrying either the actin 5′-UTR or 3′-UTR in place of those of ENO2. These constructs showed similar results (data not shown) of those using the tubulin elements, supporting the inhibiting role of the ENO2 5′-UTR in absence of the intron.

We next examined whether RFP expression from the ENO2 cassette requires the ENO2 intron specifically or merely the presence of any intron is sufficient. To this aim, we replaced the ENO2 intron in *prENO2/RFP + INT$_{ENO2}$* with the similar sized (511 bp) first intron of the tubulin gene. Parasite transfection with this construct, named *prENO2/RFP + INT$_{TUB}$*, resulted in intermediate expression of RFP (Fig. 4C), indicating that the ENO2 intron

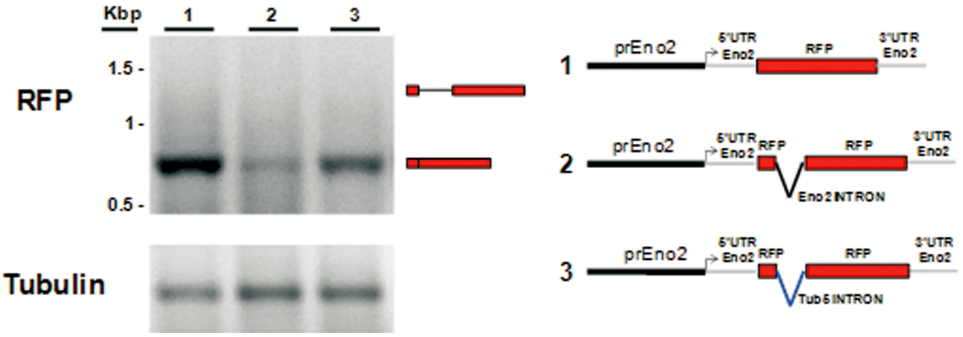

Fig. 5. The ENO2 intron affects mRNA abundance. Total RNA was isolated from tachyzoites stably transfected with *prENO2/RFP*, *prENO2/RFP + INT$_{ENO2}$* or *prENO2/RFP + INT$_{TUB}$* along with DHFR resistance plasmid. After 8 days of pyrimethamine selection, total RNAs were purified from these transgenic parasites. After *Dnase I* treatment and reverse transcription, cDNAs were analyzed by PCR using primers to detect RFP (R1F and R1R primers) or tubulin (T5F and T5R primers).

overcomes suppression more efficiently than a heterologous intron.

Moreover, the ENO2 5′-UTR was capable of suppressing RFP expression even when placed downstream of the transcription start site of the strong tubulin promoter (*pTUB/5′UTR$_{ENO2}$-RFP*, Fig. S1B). The introduction of the ENO2 intron into the RFP coding region of *pTUB/5′UTR$_{ENO2}$-RFP* restored the strong RFP synthesis typical of the tubulin promoter (Fig. S1C). These findings indicate that ENO2 5′UTR suppression of an intronless gene does not depend on promoter type.

We reasoned that suppression of RFP expression by the ENO2 5′-UTR in the absence of the intron might be due to an effect on mRNA abundance. To address this, we purified total RNA from parasites transfected with either *prENO2/RFP + INT$_{ENO2}$* or *prENO2/RFP* and, after *DNase I* treatment and reverse transcription, we analyzed the RFP cDNA abundance by PCR. As shown in Fig. 5, RFP cDNA was barely detected in parasites transfected with *prENO2/RFP* (lane 2), but was abundant in tachyzoites transfected with *prENO2/RFP + INT$_{ENO2}$* (lane 1). PCR analysis of parasites transfected with *prENO2/RFP + INT$_{TUB}$* showed intermediate abundance of the RFP product (lane 3), in accordance with the partial restoration of RFP synthesis observed by flow cytometry (Fig. 4C). Both ENO2 and tubulin introns were correctly spliced and IR was not observed in tachyzoites transfected with these constructs. Taken together, these results indicate that the ENO2 5′UTR and intron are key elements that control the expression of this gene.

Appropriate expression of ENO1 in bradyzoites requires a longer ENO1 3′-UTR, but does not require an intron

Kibe *et al*. (2005) investigated ENO1 promoter activity several years ago using CAT as a reporter to dissect the ENO1 expression unit in bradyzoites. IR observed in ENO1 transcripts in tachyzoites prompted us to revisit this gene with the intention of identifying elements involved in post-transcriptional regulation of ENO1 expression. We began this analysis by recreating the same expression cassette used by Kibe *et al*. as a starting construct. The expression cassette, named *prENO1/EGFP*, consisted of a DNA fragment spanning 1240 bp upstream of the ENO1 ATG followed by the EGFP coding region and 322 bp of the ENO1 3′-UTR. PLK parasites were transfected with *prENO1/EGFP*, drug selected for 8 days, differentiated to bradyzoites in alkaline media, and tested for EGFP expression by fluorescence microscopy (data not shown) and flow cytometry (Fig. 6B). EGFP expression was barely detectable in just a few parasites after prolonged growth in alkaline media in agreement with the very low expression level described by Kibe *et al*. (2005). Next, we wondered whether expression driven by the ENO1 promoter required the presence of its unique intron as observed in the ENO2 gene. To assess this, we placed the ENO1 intron into the EGFP coding region 40 bp upstream of the ATG, reproducing its location inside the ENO1 gene (*prENO1/EGFP + INT$_{ENO1}$*). Unlike the situation for expression of RFP with the ENO2 intron in tachyzoites, insertion of the ENO1 intron did not confer EGFP expression in bradyzoites (Fig. 6C). This unexpected result prompted us to assess whether the expression cassette lacked a crucial element. To address this point, we first enlarged the ENO1 expression cassette by replacing the 322 bp ENO1 3′-UTR with a longer segment of this genomic region spanning 1300 bp downstream of the ENO1 stop codon (*prENO1/EGFP + INT$_{ENO1}$ + ^{LNG}3′UTR$_{ENO1}$*). Parasite transfection with this new construct showed no increased EGFP expression after alkaline conversion (Fig. 6D). Surprisingly, however, the longer ENO1 3′-UTR induced EGFP expression in bradyzoites transfected with a construct (*prENO1/EGFP + ^{LNG}3′UTR$_{ENO1}$*) lacking the ENO1 intron (Fig. 6E).

To help interpret these results, we performed a semi-quantitative RT-PCR analysis of the EGFP transcripts pro-

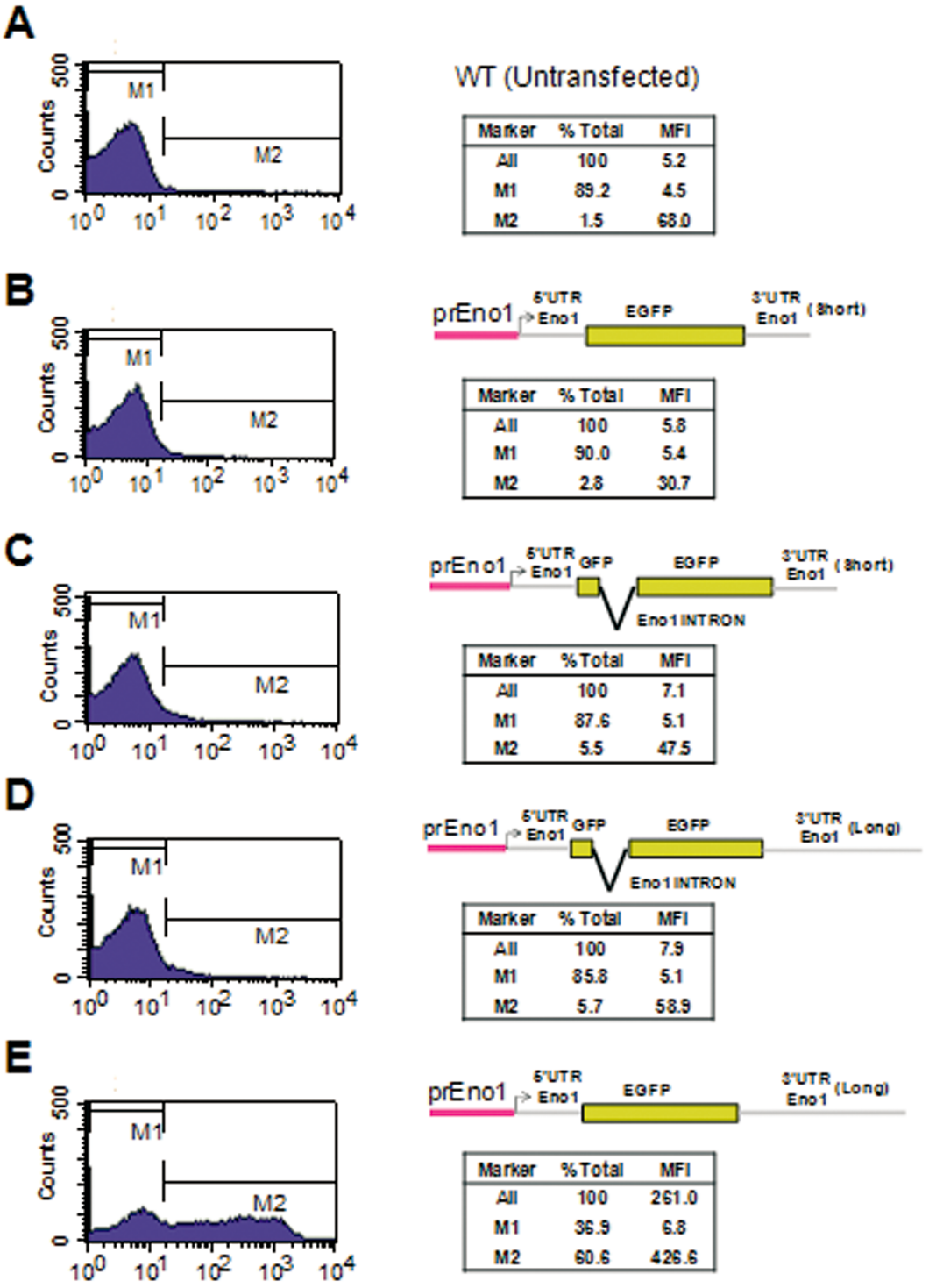

Fig. 6. EGFP expression driven by the ENO1 promoter is not restored by the ENO1 intron but requires a long 3′ UTR instead. PLK tachyzoites analyzed as WT parasites (A) or were stably transfected with *prENO1/EGFP* (B), *prENO1/EGFP* + INT_{ENO1} (C), *prENO1/EGFP* + INT_{ENO1} + $^{LNG}3'UTR_{ENO1}$ (D) or *prENO1/EGFP* + $^{LNG}3'UTR_{ENO1}$ (E) along with a DHFR resistance plasmid. After 8 days of pyrimethamine selection and 6 days of alkaline conversion, stable transfected populations were analyzed by flow cytometry. There were 50 000 events counted for each analysis. No expression was seen in tachyzoites (data not shown). Data are from one representative experiment out of three with similar results. MFI, mean fluorescence intensity.

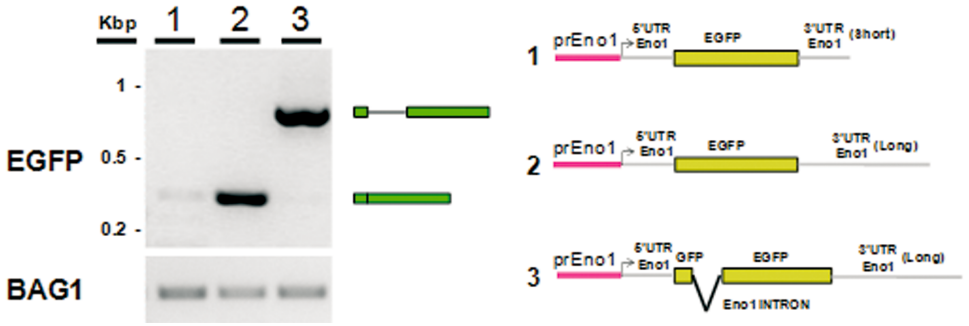

Fig. 7. Supplemental ENO1 3′-UTR sequence enhances EGFP mRNA abundance from the ENO1 promoter. Total RNA was isolated from alkaline converted parasites expressing *prENO1/EGFP* (lane 1), *prENO1/EGFP* + $^{LNG}3'UTR_{ENO1}$ (lane 2) or *prENO1/EGFP* + INT_{ENO1} + $^{LNG}3'UTR_{ENO1}$ (lane 3). After *Dnase I* treatment and reverse transcription, cDNAs were analyzed by PCR using primers to detect EGFP (EGFPF and EGFPR primers) or BAG1 (B1F and B1R primers).

duced by parasites carrying *prENO1/EGFP*, *prENO1/EGFP* + $^{LNG}3'UTR_{ENO1}$ or *prENO1/EGFP* + INT_{ENO1} + $^{LNG}3'UTR_{ENO1}$ after 6 days of bradyzoite conversion. This experiment showed that EGFP mRNA abundance was very low in parasites bearing the short ENO1 3′-UTR (Fig. 7, lane 1), but was quite abundant in parasites transfected with constructs carrying the long 3′-UTR (Fig. 7, lanes 2 and 3). Unexpectedly, the EGFP transcript derived from *prENO1/EGFP* + INT_{ENO1} + $^{LNG}3'UTR_{ENO1}$ remained unspliced, suggesting that the lack of EGFP fluorescence was due to a lack of mRNA splicing (Fig. 7, lane 3). We tested if replacing EGFP with the RFP in a new plasmid called *prENO1/RFP* + INT_{ENO1} + $^{LNG}3'UTR_{ENO1}$ resulted in a correct removal of the ENO1 intron. Like the previous EGFP construct, *prENO1/RFP* + INT_{ENO1} + $^{LNG}3'UTR_{ENO1}$ did not produce fluorescent parasites and the ENO1 intron was still not spliced (data not shown). This result suggested that the lack of intron splicing was not due to an element of the EGFP coding region that rendered the intron cryptic but that, unlike ENO2, the splicing of the ENO1 intron required supplemental sequences from its surrounding exons. Together, these findings suggest that the long 3′-UTR enhances mRNA abundance, but is insufficient to confer splicing.

To test if the ENO1 exons are required for splicing, we generated a new set of constructs in which we fused the coding region of ENO1, with or without its intron, in frame with EGFP followed by either the short or long ENO1 3′-UTR. Constructs with or without the ENO1 intron carrying the short ENO1 3′-UTR showed no ENO1-EGFP fluorescence in transfected parasites after bradyzoite conversion (Fig. 8A and B), consistent with the short 3′-UTR being insufficient to confer high mRNA abundance. As expected, the long version of the ENO1 3′-UTR conferred ENO1-EGFP expression in the absence of an intron (Fig. 8C). Interestingly, the long version of the ENO1 3′-UTR conferred ENO1-EGFP expression also when the ENO1 intron was present (Fig. 8D). These findings confirm that the long 3′UTR enhances mRNA abundance, but does not influence spicing, and they further suggest that the ENO1 exons are required for correct splicing of the intron.

To further dissect the role of the ENO1 3′-UTR on expression in bradyzoites, we asked if it functions in collaboration with the ENO1 5′-UTR. To this aim, we tested whether the ENO1 promoter still required the long ENO1 3′-UTR when the ENO1 5′-UTR is replaced with that of the tubulin gene in *prENO1/EGFP*, generating *prENO1/5′UTR*$_{TUB}$*-EGFP*. Interesting, parasites stably transfected with this construct showed a strong fluorescence after bradyzoite induction (Fig 9A, right panel). This result demonstrated that the short ENO1 3-UTR is functional and that the long 3′-UTR was only required in the presence of the ENO1 5′UTR. Moreover, EGFP expression was also slightly detectable in tachyzoites by either fluorescence microscopy (data not shown) or flow cytometry (Fig. 9A, left panel). To determine whether this leakiness was due to ENO1 promoter, we replaced it with the bradyzoite specific BAG1 promoter in *prENO1/5′UTR*$_{TUB}$*-EGFP*. We observed no detectable signal in tachyzoites transfected with this construct by fluorescence microscopy or flow cytometry (Fig. 9B, left panel), indicating that the observed leakiness is due to the ENO1 promoter and not to the tubulin 5′-UTR. Strong fluorescence was detected after bradyzoite induction (Fig. 9B, right panel). The presence of the tubulin 5′-UTR conferred stronger fluorescence to both ENO1 and BAG1 promoters compared with those carrying their own 5′ elements, indicating that the tubulin 5′-UTR bestowed more efficient translation to these transcripts.

We next investigated whether replacement of the ENO1 3′-UTR with that of tubulin was also capable of conveying EGFP expression. As shown in Fig. 10B, unlike ENO2, substitution of the ENO1 3′-UTR with that of the tubulin gene unlocked expression of EGFP. These results sug-

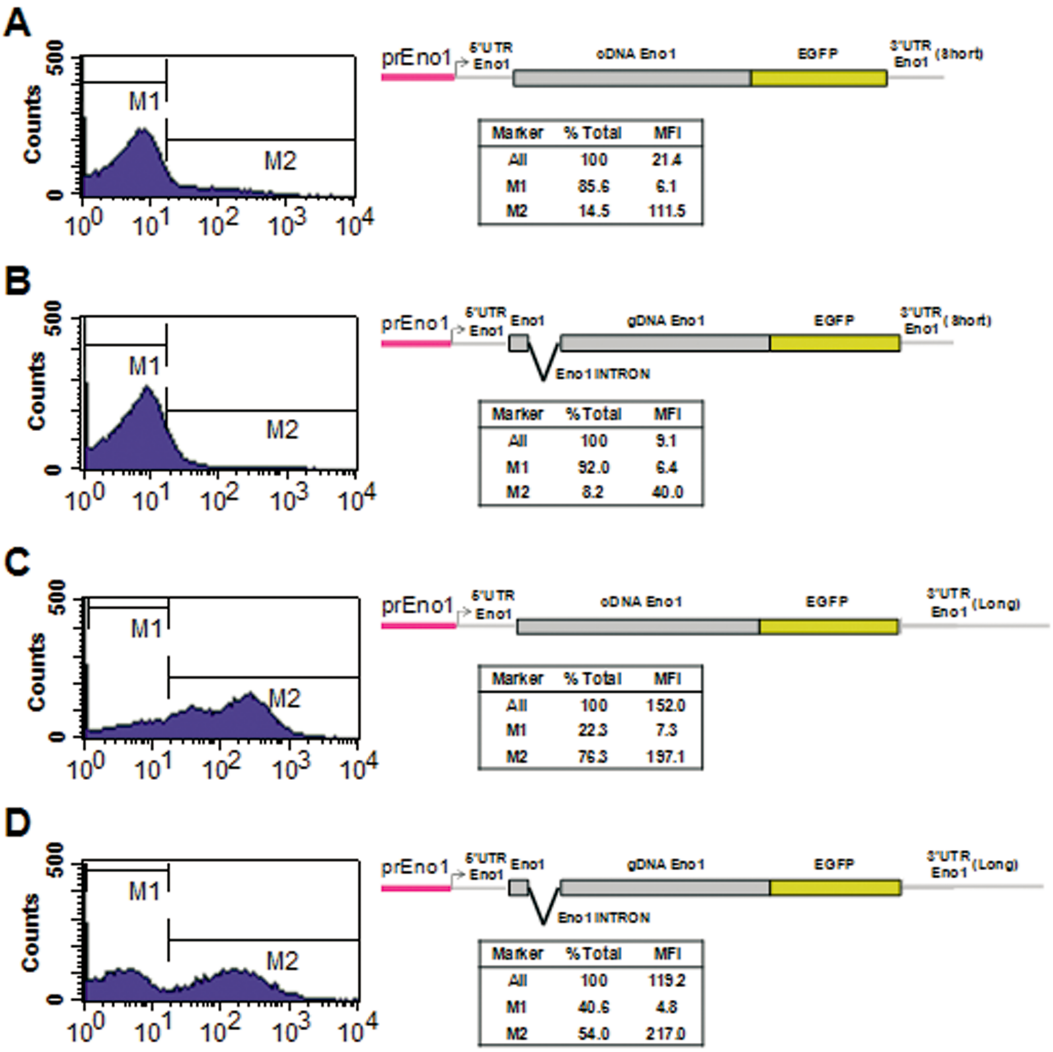

Fig. 8. ENO1 intron does not restore or enhance EGFP expression when placed in constructs carrying either the short (SHT) or long (LNG) ENO1 3′-UTR. PLK tachyzoites were stably transfected with either *prENO1/ENO1-EGFP* + $^{SHT}3'UTR_{ENO1}$ (A), *prENO1/ENO1-EGFP* + INT_{ENO1} + $^{SHT}3'UTR_{ENO1}$ (B), *prENO1/ENO1-EGFP* + $^{LNG}3'UTR_{ENO1}$ (C) or *prENO1/ENO1-EGFP* + INT_{ENO1} + $^{LNG}3'UTR_{ENO1}$ (D) along with DHFR resistance cassette. After 8 days of pyrimethamine selection and 6 days of alkaline conversion, stable transfected populations were analyzed by flow cytometry. There were 50 000 events counted for each transgenic tachyzoite/bradyzoite mixture. Untransfected alkaline-converted parasites were also analyzed to assess autofluorescence (data not shown). Data are from one representative experiment out of three with similar results. MFI, mean fluorescence intensity.

gested that sequences in both the 5′- and the 3′-UTR collaborate to license expression of ENO1 in bradyzoites.

ENO2 IR in bradyzoites is largely maintained upon expression from the ENO1 promoter

As noted above, unspliced forms of ENO2 are detectable when PLK parasites were induced to differentiate into bradyzoites with alkaline media. We wondered whether expression of the ENO2 RFP reporter cassette under the ENO1 promoter would result in fluorescent bradyzoites. To this intent, we replaced the ENO2 promoter with that of ENO1 in *prENO2/RFP* + INT_{ENO2} to generate *prENO1/5′UTR*$_{ENO2}$ + *RFP* + INT_{ENO2} + *3′UTR*$_{ENO2}$. Stably transfected parasites were induced to differentiate in bradyzoites for 6 days with alkaline media, and then analyzed by fluorescence microscopy and flow cytometry. We observed fluorescence only in a small fraction of parasites, and among them a few displayed a strong signal and the majority a mild fluorescence (Fig. 11A). The same pattern was obtained in all populations transfected with this construct in independent experiments, indicating that this bias was not due to inefficient transfection. Deletion of the ENO2 intron from *prENO1/5′UTR*$_{ENO2}$ + *RFP* + INT_{ENO2} +

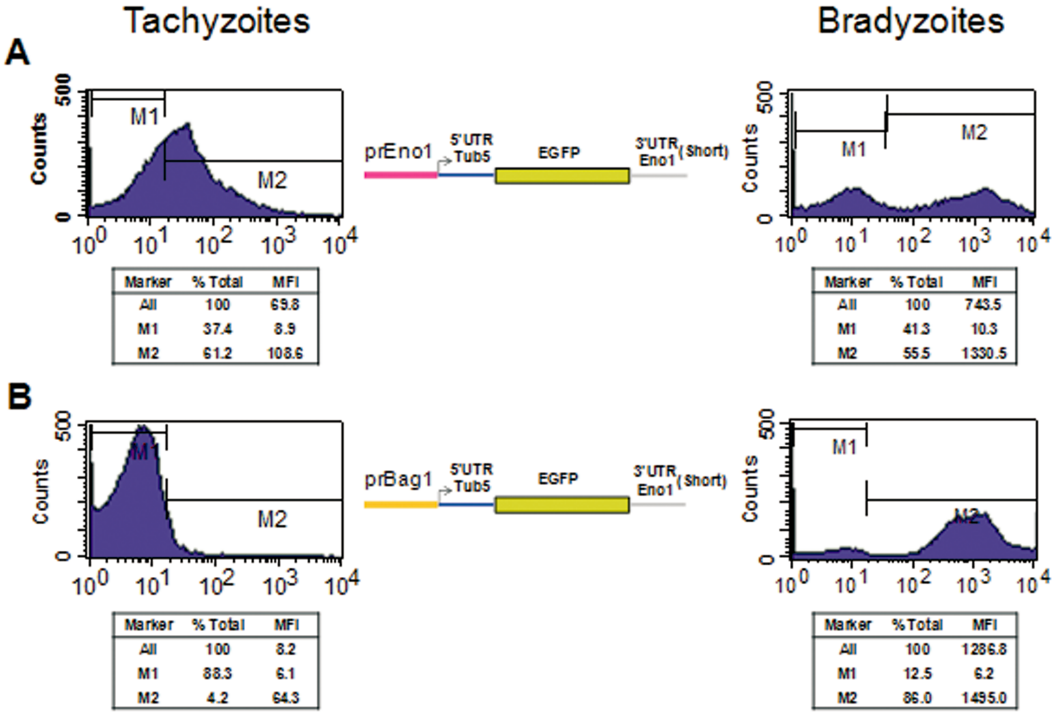

Fig. 9. Replacement of the ENO1 5′-UTR with that of tubulin restores EGFP expression in bradyzoites and shows leakiness of the ENO1 promoter in tachyzoites. PLK tachyzoites were stably transfected with either *prENO1/5′UTR$_{TUB}$-EGFP* (A) or *prBAG1/5′UTR$_{TUB}$-EGFP* (B) along with a DHFR resistance plasmid. After 8 days of pyrimethamine selection and 6 days of alkaline conversion, stable transfected populations were analyzed by flow cytometry. There were 50 000 events counted for each transgenic tachyzoite/bradyzoites mixture (right panels). The left panels show the same analysis performed on tachyzoites (100 000 events were counted). Data are from one representative experiment out of three with similar results. MFI, mean fluorescence intensity.

3′UTR$_{ENO2}$ resulted in loss of fluorescence (Fig. 11B), confirming that the intron is required when the RFP coding sequence is flanked by the ENO2 5′- and 3′-UTR.

Finally, to determine whether the low RFP expression driven by this ENO1/ENO2 chimeric transcription unit was due to intron retention, we purified RNA from *prENO2/RFP + INT$_{ENO2}$* tachyzoites or *prENO1/5′UTR$_{ENO2}$ + RFP + INT$_{ENO2}$ + 3′UTR$_{ENO2}$* bradyzoite-induced parasites to perform RT-PCR analysis. This analysis revealed that the ENO2 intron was partially retained only in parasites

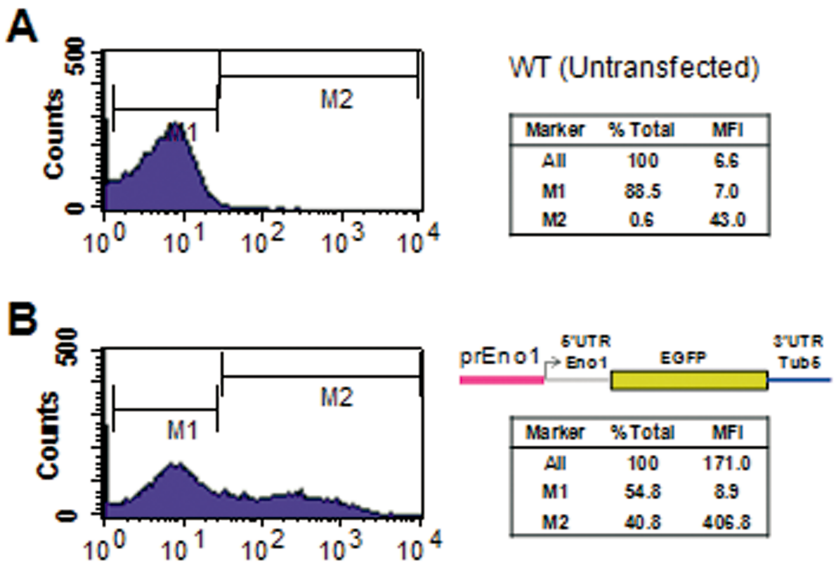

Fig. 10. Replacement of ENO1 3′-UTR with that of tubulin results in EGFP expression after alkaline conversion. Parasites stably expressing *prENO1/EGFP-3′UTR$_{TUB}$* (B) were analyzed by flow cytometry after 6 days of growth in alkaline media. Untransfected converted parasites (A) were also analyzed to assess autofluorescence. There were 50 000 events counted. Data are from one representative experiment out of three with similar results. MFI, mean fluorescence intensity.

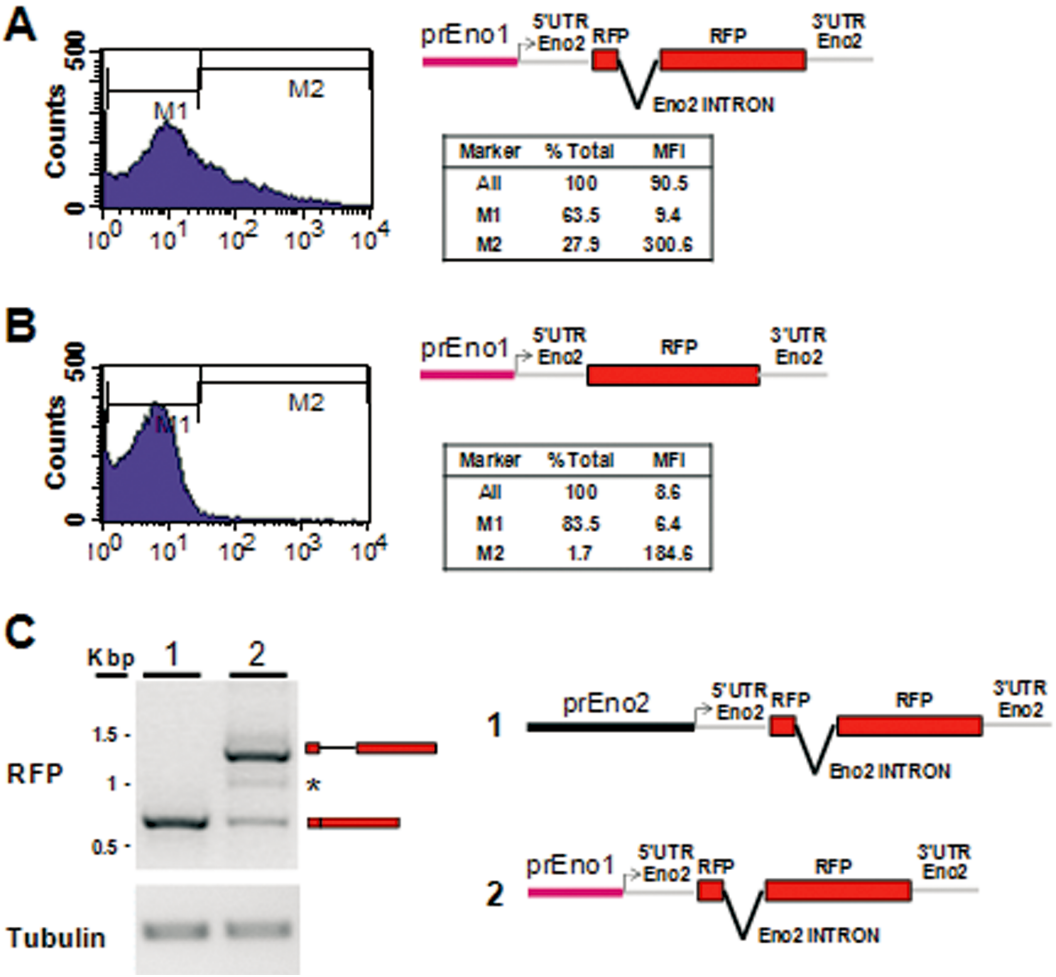

Fig. 11. ENO2 intron partially restores RFP expression in bradyzoites. *prENO1/5′UTR$_{ENO2}$ + RFP + INT$_{ENO2}$ + 3′UTR$_{ENO2}$* (A) or *prENO1/5′UTR$_{ENO2}$ + RFP+3′UTR$_{ENO2}$* (B) were stably integrated in the PLK genome by co-transfection with a DHFR resistance plasmid and 8 days of pyrimethamine selection. Tachyzoites and 6 days alkaline-converted parasites of these two transgenic strains were analyzed by flow cytometry. There were 50 000 events counted. No expression was seen in tachyzoites (data not shown). Data are from one representative experiment out of three with similar results. MFI, mean fluorescence intensity. (C) ENO2 intron is retained in the bradyzoite stage. PLK tachyzoites expressing *prENO2/RFP + INT$_{ENO2}$* were harvested and, after filter purification, used to isolate total RNA. PLK parasites stably transfected with *prENO1/5′UTR$_{ENO2}$ + RFP + INT$_{ENO2}$ + 3′UTR$_{ENO2}$* were induced to differentiate by alkaline media for 6 days and then, after syringe extrusion from HFF cells and pepsin treatment, used to purify total RNA. After treatment with *Dnase I*, both RNAs were reverse transcribed and analyzed by PCR using primers to detect either RFP (R1F and R1R) or tubulin (T5F and T5R). Lane 1: PCR performed on cDNA generated from *prENO2/RFP + INT$_{ENO2}$* tachyzoites; Lane 2: PCR performed on cDNA generated from *prENO1/5′UTR$_{ENO2}$ + RFP + INT$_{ENO2}$ + 3′UTR$_{ENO2}$* parasites after bradyzoite induction. The asterisk indicates nonspecific PCR product.

expressing RFP by ENO1 promoter after alkaline conversion (Fig. 11C, lane 2). This finding indicated that IR required factors produced only in either bradyzoites or during their conversion from tachyzoites.

Expression of the ENO *genes is not dependent on chromosomal context*

Epigenetic gene regulation has become known as a main mechanism for gene regulation in all eukaryotes. Because *T. gondii* has a full complement of histone-modifying enzymes and histones, we wondered whether the approach we used to investigate expression of *ENO* genes had hidden evidence of epigenetic regulation acting on these genes. To address this point, we exploited the availability of a type II strain carrying a deletion of the *ku80* gene (generously provided by Dr. Bzik) (Fox *et al.*, 2011). This Prugniaud Δku80 (*PruΔku80*) allows the easy targeting of selected chromosomal loci for knockouts or knockins via site-specific homologous integration. We generated new parasite strains in the *PruΔku80* background, integrating the most relevant ENO cassettes into their own original chromosomal loci by single crossover recombination (see schematic representation of the approach used in Fig. S2).

Fluorescence microscopy of single clones of *PruΔku80* carrying the RFP coding sequence under control of the most relevant ENO expression cassettes integrated in their own chromosomal loci showed fluorescence levels similar to those observed via random integration (Fig. S2). These data indicated that expression of these two stage-specific genes was mainly dependent on the intrinsic DNA sequence than epigenetic regulation. Moreover, this analysis further validated the data presented above, confirming that the UTRs and intron were key elements of the ENO transcription units.

Discussion

Tachyzoite-bradyzoite interconversion is the pivotal step that confers to *Toxoplasma* its unrivaled capacity to persist inside its host lifelong. The mechanisms governing tachyzoite-bradyzoite interconversion remain poorly understood. Differentiation, which results in cyst formation mainly in muscles and brain, is accompanied by changes in expression of glycolytic enzymes, including ENOs and LDHs. Differential expression of these glycolytic enzymes may be required to respond to biochemical and metabolic differences between the rapidly dividing tachyzoite and the slow-growing bradyzoite (Weiss and Kim, 2013). Mouveaux and colleagues recently showed that *ENO* genes are capable of binding chromatin to alter expression of a broad set of genes (Mouveaux *et al*., 2014). Moreover, the authors showed that ENO1 ablation resulted in a decrease of brain cyst burden in infected mice. Thus, a rapid exchange of the ENO protein expressed by parasites may determine the activation of genes that induce differentiation. In this study, we identified unspliced forms of ENO and LDH transcripts in parasites that are in the process of stage conversion. The ENO1 gene was reported to be exclusively expressed during the bradyzoite stage (Dzierszinski *et al*., 2001). We observed that the bradyzoite-specific ENO1 transcripts are also generated during tachyzoite stage, albeit in an unspliced form, in agreement with the absence of ENO1 protein at this stage. *In vitro* and intraperitoneal PLK tachyzoites presented both forms of ENO1, spliced and unspliced. The intron-retained transcript was the most abundant, and the mature ENO1 mRNA may be derived from the low percentage of bradyzoites that spontaneously convert *in vitro* (Soete *et al*., 1993) and *in vivo* (Di Cristina *et al*., 2008). Accordingly, the ENO1 intron-retained transcript was the only form detected in RH tachyzoites, a strain of *Toxoplasma* that exhibits low bradyzoite conversion capacity. Moreover, the immature form of ENO1 was never detected in samples prepared from PLK cysts purified from mouse brain, thus indicating that the intron is retained in tachyzoites exclusively or during the early transition toward the bradyzoite stage.

Toxoplasma ENO1 and ENO2 genes are differentially expressed in bradyzoites and tachyzoites respectively. Between these two glycolytic isoforms of ENO, ENO2 displays the highest enzymatic activity in accordance with the high metabolism of rapidly multiplying tachyzoites. Like ENO1, we observed unspliced transcripts of ENO2 only during a developmental transition, in this case from bradyzoites to tachyzoites. ENO2 intron-retention was never observed in RT-PCR experiments using PLK brain cysts, *in vitro* tachyzoites or peritoneal tachyzoites as source of RNA. IR is part of a wider process called alternative splicing, one of the main mechanisms responsible for increasing the diversity and complexity of genomes (Zhan, 2013). Splicing events such as exon skipping, truncation, extension, cryptic exons, and IR have been observed in many genes of several organisms, particularly in higher multicellular organisms. IR, which is the least characterized form of alternative splicing, consists of the complete retention of an intron in a mature transcript. IR is often associated with failure of the recognition of weak splice sites flanking short introns. Although alternative splicing is rare in protozoa, IR is the most prevalent type in such organisms (Kim *et al*., 2008; Keren *et al*., 2010). IR can result in insertion of premature stop codons (PTC) in some transcripts that are then degraded by nonsense mediated decay (NMD). Hence, IR can decrease mRNA abundance via a mechanism that has been called 'Regulated Unproductive Splicing and Translation' (RUST), which regulates expression of a broad number of genes in many organisms (Lareau *et al*., 2007). *ENO* genes contain a single intron just downstream of the ATG that introduces a stop codon in the reading frame. However, these immature transcripts are likely insensitive to NMD due to the lack of a downstream exon junction complex. Another mechanism activated by IR blocks export of unspliced pre-mRNAs from the nucleus to the cytoplasm, thus preventing their translation into aberrant polypeptides (Chang and Sharp, 1989; Legrain and Rosbash, 1989). Restriction in the nuclei usually results in degradation of the immature transcripts by the nuclear exosome machinery.

Unspliced forms of ENO transcripts may allow for rapid expression of the appropriate new stage-specific glycolytic enzyme during differentiation. In this model, low gene expression and retention of the intron could prevent untimely production of the ENO enzyme until a differentiation signal induces or represses expression of splicing regulators that dictate the cryptic intron's fate. A similar mechanism has been described for the coordinate expression of a battery of neuronal genes during neurogenesis (Yap *et al*., 2012). Retention of an intron in the 3′-UTR of some neuronal genes by polypyrimidine tract-binding protein (Ptbp1) restricted these immature transcripts to the nucleus, leading to their degradation by the nuclear RNA surveillance machinery. Decreased expression of Ptbp1

during neuronal differentiation allows intron splicing and accumulation of translation-competent mRNAs in the cytoplasm. Other genes regulated by similar mechanisms are those coding for proinsulin (Mansilla *et al*., 2005), cyclooxygenase-1 (Cui *et al*., 2004; Qin *et al*., 2005), mitochondrial transcription termination factor (Li *et al*., 2005) and gonadotropin-releasing hormone (Seong *et al*., 1999), among others. The serine- and arginine-rich protein SF2/ASF (Sun *et al*., 2010) autoregulates its expression by repressing the splicing of some of its introns, while apolipoprotein E (APOE; Xu *et al*., 2008) retains intron 3 specifically in neuron cells restricting the transcripts in the nucleus. The splicing of APOE intron 3 is induced in response to excitotoxic stimuli to increase APOE expression. Intron-containing transcripts retained in the nucleus are thus usually targeted to the nuclear exosome for degradation, although several reports described different fates of these immature messengers. For example, Hett and West (2014) showed that the pre-mRNAs produced following U4 snRNA inhibition were stable in the nucleus and that nuclear RNA degradation factors did not relocalize to nuclear speckles following splicing inhibition. Moreover, the pre-mRNAs remained competent for splicing after removing the U4 snRNA inhibition. Denis *et al*. (2005) reported that interleukin-1 is a component of a subset of pre-mRNAs that retained introns in mature human platelets. The retained intron of interleukin-1 pre-mRNAs was spliced to generate mature transcripts, leading to new synthesis of IL-1β protein in response to cellular activation. These studies indicate that IR can function as a time-regulated mechanism to forestall translation and accumulate preformed, but translationally incompetent unspliced transcripts, that cells may utilize at specific developmental stages. In this work, we have not investigated whether the immature forms of *ENO* genes identified during the tachyzoite-bradyzoite interconversion process were subject of either delayed splicing and then translation or degradation. However, because proteins are synthesized more rapidly from preexisting stored mRNAs than from genes that require transcriptional activation, it can be hypothesized that parasites might utilize a developmental regulated splicing of these transcripts to promptly provide initial stage-specific ENO to enter differentiation before upregulating the ENO promoters. Similar to *ENO* genes, we identified retained introns in LDH transcripts, suggesting that parasites may utilize this mechanism to tightly control stage-specific expression. However, unspliced forms of *LDH* genes were barely detectable by RT-PCR, indicating that production of these immature forms was very low during interconversion compared to *ENO* genes.

Dissection of the elements composing the ENO transcription units allowed the identification of regions that regulate ENO expression. To perform this analysis, we generated several constructs bearing combinations of the *ENO* gene elements. Although variables such as transfection efficiency, vector genome locus integration and bradyzoite conversion efficiency were limitations, our approach nevertheless allowed the identification of ENO elements playing roles in transcriptional and posttranscriptional processes. As for the ENO2 transcriptional unit, efficient synthesis of fluorescent reporter was only observed when the intron was introduced inside the RFP coding sequence. The intron was only required when the ENO2 5′-UTR was present, indicating that these two elements were in some way coupled, perhaps to control temporal splicing of the transcripts. In the absence of the intron, the ENO2 promoter drove reporter production, providing that the 5′-UTR was replaced with that of another gene such as tubulin or actin. The ENO2 3′-UTR seemed to play no other role than to terminate transcription. The introduction of the tubulin intron partially restored expression of RFP, suggesting that factors binding the ENO2 5′-UTR may interact with the splicing machinery. Moreover, ENO2 5′-UTR was capable of inhibiting expression driven by promoters other than ENO2, such as tubulin. Repression was released by introducing the ENO2 intron in this construct, confirming that these two elements were interacting together in some way. We have not investigated the nature of the repression carried out by the ENO2 5′-UTR, but we hypothesize that may occur by inhibiting nuclear export in absence of splicing, thus leading to rapid degradation of the transcripts. This hypothesis is in accordance with the very low abundance of RFP transcripts detected by RT-PCR, although we cannot rule out destabilization of cytoplasmic transcripts carrying the ENO2 5′-UTR that did not go through the splicing machinery. Retention of the ENO2 intron was only observed when the RFP coding sequence, embedded into the ENO2 5′-UTR and intron, was expressed in the bradyzoite stage by exploiting the stage specificity of the ENO1 promoter. We observed only partial ENO2 IR with part of the transcripts fully mature. This result suggests that IR is likely due to the presence of limiting amounts of splicing regulators, in accordance with low abundance of ENO transcripts during early differentiation.

In contrast, an analysis of the ENO1 transcription unit highlighted that the 5′- and 3′-UTR interacted and the intron was not essential to generate fluorescence from the ENO1 promoter after parasite conversion into bradyzoites. The ENO1 intron was not spliced when placed inside the reporter coding sequence, as occurred for ENO2 intron, indicating that exonic splicing enhancers (ESEs) may be required for splicing this intron. Replacing the 5′ or 3′-UTR with those from other genes such as tubulin resulted in reporter expression. The ENO1 3′-UTR required a supplemental sequence when coupled to its 5′-UTR, whereas the shorter ENO1 3′-UTR was fully functional in the presence of a heterologous 5′-UTR. Although difficult to interpret with

the current information, we speculate that the 5′-UTR may bind a factor(s) that interact directly or indirectly to sequences of the longer ENO1 3′-UTR, perhaps to regulate temporal intron splicing. That the short version of the ENO1 3′-UTR inhibited EGFP expression only when coupled with the ENO1 5′-UTR suggests these two UTR elements interact. Further, the lack of a supplemental sequence might have caused this interaction to exert an inhibition on EGFP expression, perhaps due to factors assembled improperly on the 5′- and 3′-UTR. Like ENO2 intron-less transcripts, we found very low abundance of reporter transcripts when the short version of ENO1 3′-UTR was placed in the construct. Introns and UTR elements have been found to cooperatively dictate expression of some proteins. For example, an intron present within the 5′-UTR of the *Drosophila* male-specific-lethal 2 (msl-2) mRNA is alternatively spliced in a sex-specific fashion such that the intron is removed in males, but retained in females (Salz and Erickson, 2010). The msl-2 intron contains two binding sites for Sex-lethal (SXL), an RNA binding protein known to regulate pre-mRNA splicing (Cline, 1993; Baker *et al*., 1994). One binding site is located adjacent to the 5′ splice site and the other is just upstream of the 3′ splice site. The SXL binding sites retained within this intron in the 5′-UTR, combined with additional SXL binding sites located in the 3′-UTR, are bound by SXL to inhibit translation of msl-2 mRNA (Abaza *et al*., 2006).

Results obtained above were also validated using another strain, Pru*Δku80*, that allows site-specific integration of exogenous DNA. The most informative ENO expression cassettes were integrated in their loci by single crossing-over events, and single parasite clones were analyzed by fluorescence microscopy. The impact on RFP expression by the elements composing the ENO transcription units, UTRs and introns, was comparable with that already observed from random integration of the constructs carried out with the ME49 strain. These results indicate that expression of these transcription units were not dependent by locus-specific epigenetic marks.

Taken together, our findings may account for the fine regulation of the *ENO* genes reported above, in which coupled elements of their transcripts (5′-UTR and intron in ENO2; 5′-UTR and 3′-UTR in ENO1) may interact together by binding factors involved in the regulated removal of the introns in response of environmental signals. In this work, we have not explored whether these elements bind proteins. This will be the subject of future investigations. It is conceivable that exploiting these sequences will identify factors that control the regulated splicing of ENO transcripts during tachyzoite-bradyzoite interconversion. Identification of proteins controlling these events will be fundamental to understanding stage differentiation in *Toxoplasma*.

Experimental procedures

Host cells and parasite cultures

Human foreskin fibroblasts (HFFs) were grown in Dulbecco's modified Eagle's medium (Invitrogen) containing 10% fetal bovine serum (Invitrogen). A single *T. gondii* line, the clonal isolate PLK of the ME49 strain, was used in all genetic manipulations described here. The clonal isolate EP of the RH strain was also used in this study. Parasites were propagated *in vitro* by serial passage on monolayers of HFF (Roos *et al*., 1994). *In vivo* PLK tachyzoites were obtained by phosphate-buffered saline (PBS) lavage of the intraperitoneal (i.p.) cavity of Swiss-CD1 mice (5 weeks old; Harlan Sprague-Dawley) 4 days postinfection with 10^4 tachyzoites by i.p. injection.

Cyst purification

Swiss-CD1 mice (5 weeks old; Harlan Sprague-Dawley) were inoculated with 10^4 PLK tachyzoites by i.p. injection. Mouse brains were harvested at 5 weeks postinfection and homogenized in 2 ml of PBS by syringe passage through a 19-gauge needle. Cysts were purified from brain by isopycnic centrifugation as previously described (Cornelissen *et al*., 1981; Weiss *et al*., 1992). Release of bradyzoites from purified cysts was carried out by incubating purified cysts in 170 mM NaCl/pepsin (0.1 mg ml^{-1})/60 mM HCl for 30 min at 37°C. Total RNA was extracted from released bradyzoites using the RNeasy minikit (Qiagen), and 1 μg of RNA was reverse transcribed using the SuperScript III first-strand synthesis system (Invitrogen) for RT-PCR.

T. gondii *transfection experiments*

Freshly harvested tachyzoites (2×10^7) were centrifuged to remove the culture medium, and the resulting pellet was resuspended in cytomix [120 mM KCl, 0.15 mM $CaCl_2$, 10 mM K_2HPO_4-KH_2PO_4 (pH 7.6), 25 mM HEPES (pH 7.6), 2 mM EGTA, 5 mM $MgCl_2$, 2 mM ATP, 5 mM glutathione]. Parasites were resuspended in 700 μl of cytomix containing 100 μg of plasmid DNA to be tested and 5 μg of pyrimethamine resistance cassette. Prior to electroporation, the two plasmids were linearized with the endonuclease *NotI* (Black *et al*., 1995). The entire mixture was then transferred to an electroporation cuvette (4-mm gap) and exposed to an electric pulse with an electroporator (BTX Electro Cell Manipulator 600) in the high-voltage mode (charging voltage and resistance set at 2.0 kV and 48 W respectively). Electroporated parasites were transferred to fresh HFF monolayers and subjected to pyrimethamine selection for 8 days prior to be analyzed by fluorescence microscopy or flow cytometry. When plasmids carrying the ENO1 promoter were used for transfection, the 8 days of pyrimethamine selection were followed by 6 days of bradyzoite conversion in alkaline media before analysis.

In vitro *conversion*

In vitro tachyzoite-to-bradyzoite conversion was induced by exposing parasite cultures to pH 8.2 as described previously

(Soete *et al.*, 1993; Weiss *et al.*, 1995; Galizi *et al.*, 2013). Briefly, bradyzoite differentiation was induced *in vitro* by culturing tachyzoite-infected cells in RPMI 1640 buffered with 50 mM HEPES to pH 8.2, in absence of CO_2, and supplemented with 3% fetal bovine serum.

RT-PCR analysis

Total RNA was extracted from parasites using the RNeasy minikit (Qiagen), and 1 μg of RNA was reverse transcribed using the SuperScript III first-strand synthesis system (Invitrogen) for RT-PCR and used as the template for each PCR (35 cycles of 95°C for 30 s, 60°C for 30 s, and 72°C for 60 s). All purified RNAs were treated with *DNase I* using TURBO DNA-free™ Kit (Invitrogen) before RT. PCRs were performed in 20 μl, and the whole reaction products were loaded on a 1% agarose gel. The primers used in these analyses are listed in Table S1.

Expression vectors

All the expression vectors were generated from the basic plasmid pBluescript II SK (Stratagene). ENO promoters were amplified from genomic DNA purified from PLK parasites and cloned in the *ApaI* and *SalI* sites upstream of either EGFP or RFP. ENO1 and ENO2 promoters were constituted by a DNA fragment spanning 1240 and 1930 bp upstream of the ATG respectively. The 3′-UTR segments of both expression cassettes were cloned in the restriction sites *PacI* and *NotI* downstream of the reporter. ENO2 3′-UTR was constituted by a DNA fragment spanning 683 bp downstream of the ENO2 stop codon. The 3′-UTR fragment used in the ENO1 vectors was composed by 322 and 1300 bp, downstream of the ENO1 stop codon, in the short and long versions of the ENO1 3′-UTR respectively. All variants of these basic vectors were achieved by overlap PCR as described by Horton *et al.* (1989). The primers used to generate all vectors are listed in Table S1. All constructs were sequenced to rule out the occurrence of nucleotide substitutions in either the promoter or the coding sequences.

Site-specific genomic integration of ENO constructs into their own loci of PruΔKu80

The strain *PruΔKu80* was employed to obtain site-specific integration of the more informative ENO constructs (Fox *et al.*, 2011). The pyrimethamine resistance cassette (*prSag1/TgDHFR/3′UTR*$_{SAG1}$) was excised from the backbone using the restriction enzymes *HindIII* and *NotI* and, after blunting the *HindIII* end by phusion treatment, cloned in the restriction sites *SpeI* (blunted by phusion treatment) and *NotI* downstream of the *prENO2/RFP*, *prENO2/RFP* + *INT*$_{ENO2}$ or *prENO2/5′UTR*$_{TUB}$*-RFP* expression cassettes. Because the *PruΔKu80* strain becomes green fluorescent after bradyzoite conversion due to the presence in its genome of the EGFP coding sequence under control of the LDH2 promoter, all the site-specific expression cassettes for analyzing the ENO1 transcription units were first genetically manipulated to replace EGFP with RFP (using the restriction sites *SalI* and *PacI*). The *prENO1/RFP*, *prENO1/RFP* + ^{LNG}*3′UTR*$_{ENO1}$ and *prENO1/5′UTR*$_{TUB}$*-RFP* expression cassettes were then excised from the backbone using the restriction enzymes *ApaI* and *NotI* and, after blunting the *NotI* end by phusion treatment, cloned in the restriction sites *ApaI* and *XhoI* (blunted by phusion treatment) upstream of the bleomycin resistance cassette (*prGra1/tnBLE/3′UTR*$_{SAG1}$). The *prENO2/RFP_TgDHFR*, *prENO2/RFP* + *INT*$_{ENO2}$*_TgDHFR* and *prENO2/5′UTR*$_{TUB}$*-RFP_TgDHFR* vectors were linearized with *NarI* to cut within the ENO2 promoter and used to transfect *PruΔKu80*. The *prENO1/RFP_ble*, *prENO1/RFP* + ^{LNG}*3′UTR*$_{ENO1}$*_ble* and *prENO1/5′UTR*$_{TUB}$*-RFP_ble* vectors were linearized with *AatII* to cut within the ENO1 promoter and used to transfect *PruΔKu80*. After selection with either pyrimethamine or bleomycin and parasite cloning by limiting dilution, genomic DNA purified from single clones was analyzed by PCR using primers designed to detect site-specific genomic integration (see Fig. S2 for the integration and PCR detection strategy).

Flow cytometry

Parasites purified for transfection were always tested for the efficiency of plasmid incorporation by setting a separate, parallel, control transfection using a vector expressing EGFP under the TUB promoter. Experiments showing < 30% cells expressing EGFP were discontinued. Transfected parasites were subjected to pyrimethamine selection for 8 days before being analyzed by flow cytometry. An analysis of *in vitro*-induced bradyzoites was performed after an additional 6 days of parasite growth in alkaline media. Intracellular parasites were harvested from *in vitro* cultures by sequential scraping, syringing and 3 μm filtering. Bradyzoites were released from *in vitro* cysts by digestion in 170 mM NaCl/pepsin (0.1 mg ml^{-1})/60 mM HCl for 30 min at 37°C and neutralization with 94 mM Na_2CO_3. Purified parasites were then analyzed using FACScan flow cytometer (Becton Dickinson, BD). Autofluorescence was assessed using untransfected parasites. For tachyzoite and bradyzoite analysis, 100 000 and 50 000 parasites were acquired respectively. The acquired data were analyzed with CELLQuest software (BD).

Acknowledgements

We thank Professor Carla Emiliani for helpful discussion of the manuscript. This work was supported by grant ELA no. 2011-037C1B and AIRC 5 per mille (2011) Pr. 12214, Fondazione Cassa di Risparmio di Perugia Grant no. 2014.0222.021 and PRIN 2010/11 no. 2010FM738P.

Conflict of interest

The authors declare to have no conflicting interests.

References

Abaza, I., Coll, O., Patalano, S., and Gebauer, F. (2006) *Drosophila* UNR is required for translational repression of male-specific lethal 2 mRNA during regulation of

X-chromosome dosage compensation. *Genes Dev* **20:** 380–389.
Al-Anouti, F., Tomavo, S., Parmley, S., and Ananvoranich, S. (2004) The expression of lactate dehydrogenase is important for the cell cycle of *Toxoplasma gondii*. *J Biol Chem* **279:** 52300–52311.
Averbeck, N., Sunder, S., Sample, N., Wise, J.A., and Leatherwood, J. (2005) Negative control contributes to an extensive program of meiotic splicing in fission yeast. *Mol Cell* **18:** 491–498.
Baker, B.S., Gorman, M., and Marin, I. (1994) Dosage compensation in *Drosophila*. *Annu Rev Genet* **28:** 491–521.
Black, M., Seeber, F., Soldati, D., Kim, K., and Boothroyd, J.C. (1995) Restriction enzyme-mediated integration elevates transformation frequency and enables co-transfection of *Toxoplasma gondii*. *Mol Biochem Parasitol* **74:** 55–63.
Bohne, W., Holpert, M., and Gross, U. (1999) Stage differentiation of the protozoan parasite *Toxoplasma gondii*. *Immunobiology* **201:** 248–254.
Boothby, T.C., Zipper, R.S., van der Weele, C.M., and Wolniak, S.M. (2013) Removal of retained introns regulates translation in the rapidly developing gametophyte of *Marsilea vestita*. *Dev Cell* **24:** 517–529.
Chang, D.D., and Sharp, P.A. (1989) Regulation by HIV Rev depends upon recognition of splice sites. *Cell* **59:** 789–795.
Cline, T.W. (1993) The *Drosophila* sex determination signal: how do flies count to two? *Trends Genet* **9:** 385–390.
Cornelissen, A.W., Overdulve, J.P., and Hoenderboom, J.M. (1981) Separation of *Isospora* (*Toxoplasma*) *gondii* cysts and cystozoites from mouse brain tissue by continuous density-gradient centrifugation. *Parasitology* **83:** 103–108.
Cui, J.G., Kuroda, H., Chandrasekharan, N.V., Pelaez, R.P., Simmons, D.L., Bazan, N.G., and Lukiw, W.J. (2004) Cyclooxygenase-3 gene expression in Alzheimer hippocampus and in stressed human neural cells. *Neurochem Res* **29:** 1731–1737.
Denis, M.M., Tolley, N.D., Bunting, M., Schwertz, H., Jiang, H., Lindemann, S., *et al*. (2005) Escaping the nuclear confines: signal-dependent pre-mRNA splicing in anucleate platelets. *Cell* **122:** 379–391.
Denton, H., Roberts, C.W., Alexander, J., Thong, K.W., and Coombs, G.H. (1996) Enzymes of energy metabolism in the bradyzoites and tachyzoites of *Toxoplasma gondii*. *FEMS Microbiol Lett* **137:** 103–108.
Di Cristina, M., Marocco, D., Galizi, R., Proietti, C., Spaccapelo, R., and Crisanti, A. (2008) Temporal and spatial distribution of *Toxoplasma gondii* differentiation into bradyzoites and tissue cyst formation *in vivo*. *Infect Immun* **76:** 3491–3501.
Dubey, J.P., Lindsay, D.S., and Speer, C.A. (1998) Structures of *Toxoplasma gondii* tachyzoites, bradyzoites, and sporozoites and biology and development of tissue cysts. *Clin Microbiol Rev* **11:** 267–299.
Dzierszinski, F., Mortuaire, M., Dendouga, N., Popescu, O., and Tomavo, S. (2001) Differential expression of two plant-like enolases with distinct enzymatic and antigenic properties during stage conversion of the protozoan parasite *Toxoplasma gondii*. *J Mol Biol* **309:** 1017–1027.
Ferguson, D.J., Parmley, S.F., and Tomavo, S. (2002) Evidence for nuclear localisation of two stage-specific isoenzymes of enolase in *Toxoplasma gondii* correlates with active parasite replication. *Int J Parasitol* **32:** 1399–1410.
Fox, B.A., Falla, A., Rommereim, L.M., Tomita, T., Gigley, J.P., Mercier, C., *et al*. (2011) Type II *Toxoplasma gondii* KU80 knockout strains enable functional analysis of genes required for cyst development and latent infection. *Eukaryot Cell* **10:** 1193–1206.
Galizi, R., Spano, F., Giubilei, M.A., Capuccini, B., Magini, A., Urbanelli, L., *et al*. (2013) Evidence of tRNA cleavage in apicomplexan parasites: half-tRNAs as new potential regulatory molecules of *Toxoplasma gondii* and *Plasmodium berghei*. *Mol Biochem Parasitol* **188:** 99–108.
Hett, A., and West, S. (2014) Inhibition of U4 snRNA in human cells causes the stable retention of polyadenylated pre-mRNA in the nucleus. *PLoS ONE* **9:** e96174.
Holmes, M., Liwak, U., Pricop, I., Wang, X., Tomavo, S., and Ananvoranich, S. (2010) Silencing of tachyzoite enolase 2 alters nuclear targeting of bradyzoite enolase 1 in *Toxoplasma gondii*. *Microbes Infect* **12:** 19–27.
Horton, R.M., Hunt, H.D., Ho, S.N., Pullen, J.K., and Pease, L.R. (1989) Engineering hybrid genes without the use of restriction enzymes: gene splicing by overlap extension. *Gene* **77:** 61–68.
Kavanagh, K.L., Elling, R.A., and Wilson, D.K. (2004) Structure of *Toxoplasma gondii* LDH1: active-site differences from human lactate dehydrogenases and the structural basis for efficient APAD + use. *Biochemistry* **43:** 879–889.
Keren, H., Lev-Maor, G., and Ast, G. (2010) Alternative splicing and evolution: diversification, exon definition and function. *Nat Rev Genet* **11:** 345–355.
Kibe, M.K., Coppin, A., Dendouga, N., Oria, G., Meurice, E., Mortuaire, M., *et al*. (2005) Transcriptional regulation of two stage-specifically expressed genes in the protozoan parasite *Toxoplasma gondii*. *Nucleic Acids Res* **33:** 1722–1736.
Kim, E., Goren, A., and Ast, G. (2008) Alternative splicing: current perspectives. *Bioessays* **30:** 38–47.
Lareau, L.F., Brooks, A.N., Soergel, D.A., Meng, Q., and Brenner, S.E. (2007) The coupling of alternative splicing and nonsense-mediated mRNA decay. *Adv Exp Med Biol* **623:** 190–211.
Legrain, P., and Rosbash, M. (1989) Some cis- and trans-acting mutants for splicing target pre-mRNA to the cytoplasm. *Cell* **57:** 573–583.
Li, X., Zhang, L.S., and Guan, M.X. (2005) Cloning and characterization of mouse mTERF encoding a mitochondrial transcriptional termination factor. *Biochem Biophys Res Commun* **326:** 505–510.
Manger, I.D., Hehl, A., Parmley, S., Sibley, L.D., Marra, M., Hillier, L., *et al*. (1998) Expressed sequence tag analysis of the bradyzoite stage of *Toxoplasma gondii*: identification of developmentally regulated genes. *Infect Immun* **66:** 1632–1637.
Mansilla, A., Lopez-Sanchez, C., de la Rosa, E.J., Garcia-Martinez, V., Martinez-Salas, E., de Pablo, F., and Hernandez-Sanchez, C. (2005) Developmental regulation of a proinsulin messenger RNA generated by intron retention. *EMBO Rep* **6:** 1182–1187.
Mouveaux, T., Oria, G., Werkmeister, E., Slomianny, C., Fox, B.A., Bzik, D.J., and Tomavo, S. (2014) Nuclear glycolytic enzyme enolase of *Toxoplasma gondii* functions as a transcriptional regulator. *PLoS ONE* **9:** e105820.

Qin, N., Zhang, S.P., Reitz, T.L., Mei, J.M., and Flores, C.M. (2005) Cloning, expression, and functional characterization of human cyclooxygenase-1 splicing variants: evidence for intron 1 retention. *J Pharmacol Exp Ther* **315:** 1298–1305.

Roos, D.S., Donald, R.G., Morrissette, N.S., and Moulton, A.L. (1994) Molecular tools for genetic dissection of the protozoan parasite *Toxoplasma gondii*. *Methods Cell Biol* **45:** 27–63.

Salz, H.K., and Erickson, J.W. (2010) Sex determination in *Drosophila*: the view from the top. *Fly (Austin)* **4:** 60–70.

Seong, J.Y., Park, S., and Kim, K. (1999) Enhanced splicing of the first intron from the gonadotropin-releasing hormone (GnRH) primary transcript is a prerequisite for mature GnRH messenger RNA: presence of GnRH neuron-specific splicing factors. *Mol Endocrinol* **13:** 1882–1895.

Soete, M., Fortier, B., Camus, D., and Dubremetz, J.F. (1993) *Toxoplasma gondii*: kinetics of bradyzoite-tachyzoite interconversion in vitro. *Exp Parasitol* **76:** 259–264.

Soldati, D., and Boothroyd, J.C. (1995) A selector of transcription initiation in the protozoan parasite *Toxoplasma gondii*. *Mol Cell Biol* **15:** 87–93.

Sun, S., Zhang, Z., Sinha, R., Karni, R., and Krainer, A.R. (2010) SF2/ASF autoregulation involves multiple layers of post-transcriptional and translational control. *Nat Struct Mol Biol* **17:** 306–312.

Tomavo, S. (2001) The differential expression of multiple isoenzyme forms during stage conversion of *Toxoplasma gondii*: an adaptive developmental strategy. *Int J Parasitol* **31:** 1023–1031.

Weiss, L.M., and Kim, K. (2000) The development and biology of bradyzoites of *Toxoplasma gondii*. *Front Biosci* **5:** D391–D405.

Weiss, L.M., and Kim, K., (2013) *Toxoplasma Gondii: The Model Apicomplexan – Perspectives and Methods*. London, UK: Academic press, Elsevier. p. xxi.

Weiss, L.M., LaPlace, D., Tanowitz, H.B., and Wittner, M. (1992) Identification of *Toxoplasma gondii* bradyzoite-specific monoclonal antibodies. *J Infect Dis* **166:** 213–215.

Weiss, L.M., Laplace, D., Takvorian, P.M., Tanowitz, H.B., Cali, A., and Wittner, M. (1995) A cell culture system for study of the development of *Toxoplasma gondii* bradyzoites. *J Eukaryot Microbiol* **42:** 150–157.

Xu, Q., Walker, D., Bernardo, A., Brodbeck, J., Balestra, M.E., and Huang, Y. (2008) Intron-3 retention/splicing controls neuronal expression of apolipoprotein E in the CNS. *J Neurosci* **28:** 1452–1459.

Yahiaoui, B., Dzierszinski, F., Bernigaud, A., Slomianny, C., Camus, D., and Tomavo, S. (1999) Isolation and characterization of a subtractive library enriched for developmentally regulated transcripts expressed during encystation of *Toxoplasma gondii*. *Mol Biochem Parasitol* **99:** 223–235.

Yang, S., and Parmley, S.F. (1995) A bradyzoite stage-specifically expressed gene of *Toxoplasma gondii* encodes a polypeptide homologous to lactate dehydrogenase. *Mol Biochem Parasitol* **73:** 291–294.

Yang, S., and Parmley, S.F. (1997) *Toxoplasma gondii* expresses two distinct lactate dehydrogenase homologous genes during its life cycle in intermediate hosts. *Gene* **184:** 1–12.

Yap, K., Lim, Z.Q., Khandelia, P., Friedman, B., and Makeyev, E.V. (2012) Coordinated regulation of neuronal mRNA steady-state levels through developmentally controlled intron retention. *Genes Dev* **26:** 1209–1223.

Zhan, L.-L. (2013) Recent advances of studies on alternative intron retention. *Trends Evol Biol* **5:** 6.

Supporting information

Additional supporting information may be found in the online version of this article at the publisher's web-site.